

<https://doi.org/10.1038/s42003-024-06924-w>

Interplay between preclinical indices of obesity and neural signatures of fluid intelligence in youth

Check for updates

Thomas W. Ward ^{1,2,3,8}, Mikki Schantell ^{1,2,4,8}, Sarah M. Dietz ^{1,2}, Grace C. Ende ^{1,2}, Danielle L. Rice ^{1,2}, Anna T. Coutant ^{1,2}, Yasra Arif ^{1,2}, Yu-Ping Wang ⁵, Vince D. Calhoun ⁶, Julia M. Stephen ⁷, Elizabeth Heinrichs-Graham ^{1,2,3}, Brittany K. Taylor ^{1,2,3} & Tony W. Wilson ^{1,2,3,4}

Pediatric obesity rates have quadrupled in the United States, and deficits in higher-order cognition have been linked to obesity, though it remains poorly understood how deviations from normal body mass are related to the neural dynamics serving cognition in youth. Herein, we determine how age- and sex-adjusted measures of body mass index (zBMI) scale with neural activity in brain regions underlying fluid intelligence. Seventy-two youth aged 9–16 years underwent high-density magnetoencephalography while performing an abstract reasoning task. The resulting data were transformed into the time-frequency domain and significant oscillatory responses were imaged using a beamformer. Whole-brain correlations with zBMI were subsequently conducted to quantify relationships between zBMI and neural activity serving abstract reasoning. Our results reveal that participants with higher zBMI exhibit attenuated theta (4–8 Hz) responses in both the left dorsolateral prefrontal cortex and left temporoparietal junction, and that weaker temporoparietal responses scale with slower reaction times. These findings suggest that higher zBMI values are associated with weaker theta oscillations in key brain regions and altered performance during an abstract reasoning task. Thus, future investigations should evaluate neurobehavioral function during abstract reasoning in youth with more severe obesity to identify the potential impact.

Pediatric obesity has become so widespread that the World Health Organization has deemed it one of this century's most momentous public health obstacles¹. In the United States, the prevalence of pediatric obesity has nearly quadrupled since the early 1970s^{2,3}. Obesity is not only a chronic disease but is also a risk factor for the development of multiple metabolic and cardiovascular diseases, including diabetes, hypertension, liver disease, kidney disease, and some cancers^{4,5}. Further, obesity early in life has been associated with an increased risk for premature death^{6–10} and has been linked to alterations in structural and functional brain development. In terms of brain structure, reductions in microstructural integrity are commonly identified in youth with overweight and obesity, though some studies report conflicting results^{11–16}. Further, obesity has been associated with cortical thinning in prefrontal regions that are crucial for executive functions and higher-order cognitive abilities, which develop across childhood and into

early adulthood^{17–19}. Executive function, which is comprised of the integration, manipulation, and inhibition of multiple cognitive processes in the pursuit of goal-directed behavior^{20,21}, emerges in early infancy, and is refined across a protracted developmental course continuing into early adulthood^{22–24}. Deficits in executive function have been implicated in both adult^{25–28} and pediatric^{11,12,15,29,30} participants with obesity and overweight. Recent reviews summarizing the pediatric obesity literature report that inhibitory control has been the most commonly studied constituent of executive function^{31–33}, though several studies have investigated working memory, cognitive flexibility, and attention and found significant associations with obesity. A considerable proportion of meta-analyses and other studies report deficits across a variety of executive functions in youth with obesity^{34–37}, though a handful of studies report conflicting results^{38–40}.

¹Institute for Human Neuroscience, Boys Town National Research Hospital, Boys Town, NE, USA. ²Center for Pediatric Brain Health, Boys Town National Research Hospital, Boys Town, NE, USA. ³Department of Pharmacology & Neuroscience, Creighton University, Omaha, NE, USA. ⁴College of Medicine, University of Nebraska Medical Center, Omaha, NE, USA. ⁵Department of Biomedical Engineering, Tulane University, New Orleans, LA, USA. ⁶Tri-institutional Center for Translational Research in Neuroimaging & Data Science (TReNDS), Georgia State University, Georgia Institute of Technology, Emory University, Atlanta, GA, USA. ⁷Mind Research Network, Albuquerque, NM, USA. ⁸These authors contributed equally: Thomas W. Ward, Mikki Schantell. ✉ e-mail: tony.wilson@boystown.org

Fluid intelligence (*Gf*) is tightly coupled with executive functions, particularly working memory and inhibitory control^{41,42}, and is more generally believed to index an individual's capacity for decontextualized reasoning and one's ability to react and adapt to novel situations or stimuli^{43,44}. *Gf* rapidly develops in childhood and has been shown to be strongly predictive of academic achievement^{45–47}. Interestingly, alterations in the development of *Gf* abilities have been associated with childhood obesity. Specifically, in a sample of 5–12 year-old children who underwent the Raven's Progressive Matrices test⁴⁸, those with severe obesity were twice as likely to have below-average *Gf* compared to normal-weight children⁴⁹. Further, in a subsample of adults from the UK Biobank study, the excess accumulation of both visceral and non-visceral (e.g., subcutaneous) adiposity was found to be inversely associated with *Gf*^{50,51}, thus underscoring the importance of additional work investigating the mechanisms giving rise to obesity-related alterations in neural and cognitive development.

Though *Gf* and higher-order cognition more broadly relies on normal functioning of prefrontal and parietal regions, Jung and Haier⁵² proposed that such functions involve a much wider set of regions in their parieto-frontal integration theory (P-FIT) of intelligence. This predominant theory of the neural basis of intelligence suggests that intelligence and reasoning are not dependent upon the activity of discrete brain regions, but instead rely upon a distributed network extending from the primary sensory cortices to the parietal, frontal, and cingulate regions to quickly and accurately transmit information to support goal-oriented behavior^{52–54}. Within these broad regions, areas of the lateral prefrontal cortex, angular gyrus, and superior and inferior parietal cortices have been frequently implicated in fMRI studies evaluating higher-order cognitive abilities, such as working memory, matrix reasoning, and card sorting tasks^{55–57}. Further, studies using magneto- and electroencephalography (M/EEG) have illuminated the crucial role that neural oscillations in parietal and prefrontal regions play in abstract reasoning^{47,58–60}. For example, a previous MEG study of abstract reasoning in adults found that older age was associated with stronger alpha/beta activity in the parietal cortices, and that functional alpha/beta connectivity was stronger with older age between the frontal and parietal cortices and weaker between parietal-hippocampal regions, thus reflecting aging-related changes in processing speed and efficiency⁶¹. There are also pediatric MEG studies of abstract reasoning showing that beta activity in frontal and temporal regions becomes stronger with development, possibly reflecting the refinement of other cognitive processes supporting *Gf* such as top-down attentional control^{47,62,63}. Perhaps most importantly, longitudinal MEG work has shown that increases in the strength of theta oscillations in prefrontal and superior temporal cortices scale with improvements in abstract reasoning performance in children and adolescents⁴⁷. More broadly, similar to other higher-order processes, greater task complexity and cognitive exertion have been linked to stronger oscillatory responses associated with abstract reasoning in the aforementioned regions^{64–66}.

With the rise in the prevalence of pediatric obesity over the last several decades, it is becoming increasingly necessary to investigate the implications not only to long-term physical health, but also to mental and cognitive

health. As previously discussed, obesity has been related to significant aberrations in cognitive processes, but less is known about its relationship with the neural mechanisms serving cognition in pediatric samples. Herein, we sought to identify whether the neural oscillatory dynamics underlying *Gf* scale with age- and sex-standardized measures of body mass index (BMI) using an abstract reasoning task and high-density MEG imaging in a community sample of children and adolescents. Of note, we focused on age- and sex-standardized measures of BMI in this study because, unlike in adult samples, the relationship between BMI and adiposity changes throughout development, which necessitates an age- and sex-corrected adjustment to BMI values⁵⁷. To mitigate this, BMI percentiles standardized for age and sex are typically used to quantify obesity in children^{68,69}, and the Center for Disease Control and Prevention (CDC) defines pediatric obesity as a BMI at or above the 95th percentile for the individual's sex and age. Based on the extant literature, we hypothesized that participants with higher age- and sex-corrected BMIs would exhibit proportional alterations in the neural oscillations serving abstract reasoning in the prefrontal and parietal cortices, and that these effects would be related to observable differences in task performance. In line with this, we find that participants with higher zBMI exhibit weaker theta oscillations and altered patterns of functional connectivity in key brain regions involved in abstract reasoning.

Results

Following parental informed consent and assent of the participating child/adolescent, all participants completed a thorough intake interview where they provided demographic, physical, and mental health information through a series of assessments and questionnaires. They then completed a custom abstract reasoning task based on Raven's Progressive Matrices (Fig. 1)^{48,70} during high-density MEG and underwent a high-resolution structural MRI scan. The MEG data were coregistered to the MRI data, transformed into time-frequency space, and significant oscillatory responses were imaged using a beamforming approach. Whole-brain correlations with zBMI were then computed across the whole sample to identify oscillatory responses that were related to zBMI. Associations with behavioral and cognitive performance were also assessed, as was functional connectivity among regions exhibiting significant relationships to zBMI. For a thorough overview of the study protocol, abstract reasoning task, and analytic pipeline, please refer to the Methods section.

Participant characteristics, neuropsychological, and behavioral results

Seventy-two youth between the ages of 9–16 years were enrolled and a total of 66 participants successfully completed the abstract reasoning task and had complete data on height, weight, sex, age, and mental health measures (Table 1; see Supplementary Table 1 for a breakdown by weight class). The sample had an average age of 13.09 years (SD = 1.93 years) and 53% were female. Participants had an average zBMI of -0.05 (SD = 1.21). As expected, age was not associated with zBMI ($r(64) = 0.12$, 95% CI: -0.12 , 0.36 , $p = 0.322$), and there were no differences in zBMI among males and females

Fig. 1 | Abstract reasoning task paradigm. Participants were presented with an empty grid of gray boxes for 2500 to 3000 ms with either the left or right bottom square highlighted by a white border to indicate the location of the upcoming target. Complex images then populated each of the four squares within the grid for 4000 ms. Participants indicated whether the image in the highlighted square correctly completed the pattern in the grid by responding via button press (i.e., right index finger for matching patterns, 60 trials; right middle finger for non-matching patterns, 60 trials). Match and non-match trials of each pattern were presented in a pseudo-randomized order for the duration of the task.

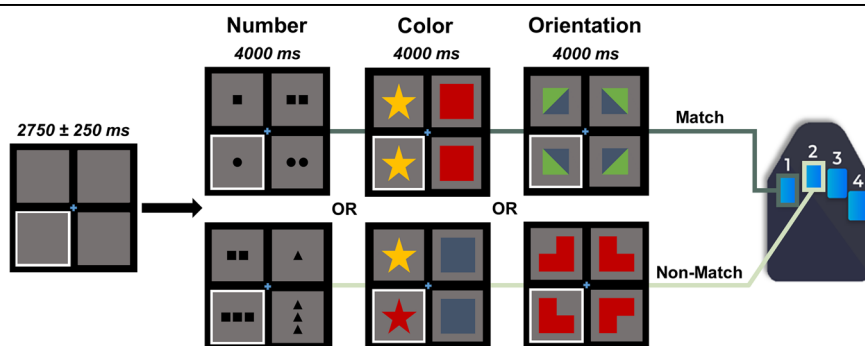


Table 1 | Participant characteristics

		Full Sample (n = 66)
Demographic Characteristics	Age (years)	13.09 (1.93)
	Sex at Birth (Male/Female)	31 Males/35 Females
	Race	61 white/1 Asian/4 More than one race
	Ethnicity	4 Hispanic or Latino/60 Not Hispanic or Latino/2 Not reported
	zBMI	-0.05 (1.21)
	Socioeconomic Status ^a	47.62 (11.08)
	Food Insecurity ^a	0.43 (1.17)
WASI-II	Perceptual Reasoning Composite (standard score) ^a	110.75 (14.32)
	Block Design (T-score)	56.05 (10.49)
	Matrix Reasoning (T-score) ^a	56.77 (7.94)
	Verbal Composite (standard score) ^a	111.80 (14.95)
	Vocabulary (T-score) ^a	57.42 (10.22)
	Similarities (T-score) ^a	57.23 (9.33)
	Full Scale IQ 4 Composite (standard score) ^a	112.77 (13.63)
Task Behavior	Accuracy (% correct)	82.55% (8.48)
	Reaction Time (ms)	1960.43 (315.43)
	Reaction Time Variability (coefficient of variation)	0.35 (0.04)
Child Behavior Checklist (CBCL) Scales	Anxious/Depressed (T-score)	51.85 (3.56)
	Withdrawn/Depressed (T-score)	52.09 (3.96)
	Somatic Complaints (T-score)	52.73 (4.39)
	Social Problems (T-score)	50.79 (1.90)
	Thought Problems (T-score)	52.03 (3.63)
	Attention Problems (T-score)	51.17 (1.67)
	Rule-Breaking Behavior (T-score)	51.00 (1.66)
	Aggressive Behavior (T-score)	50.92 (1.96)
	Internalizing Behavior (T-score)	44.95 (8.59)
Externalizing Behavior (T-score)	42.45 (7.23)	

Means and standard deviations (SD) are displayed for all continuous variables and counts are shown for all categorical variables. T-scores have a mean of 50 and a SD of 10, standard scores have a mean of 100 and a SD of 15. Higher T-scores and standard scores on the Wechsler Abbreviated Scale of Intelligence, 2nd Edition (WASI-II) subtests and scales are indicative of better cognitive functioning. Higher T-scores on the Child Behavior Checklist (CBCL) are indicative of greater clinical symptomatology.

^aData were not collected for one participant.

($t(64) = 0.69$, 95% CI: -0.39 , 0.81 , $p = 0.493$). Overall, participants performed well on the abstract reasoning task in terms of accuracy 82.55% (SD = 8.48%) and mean reaction time 1960.43 ms (SD = 315.43 ms). In terms of task behavior, we found that higher accuracy during the abstract reasoning task was significantly associated with scores on the Wechsler Abbreviated Scale of Intelligence – 2nd Edition (WASI-II), including T-scores from the Block Design subtest ($r(64) = 0.33$, 95% CI: 0.10 , 0.53 , $p = 0.007$; Fig. 2A) and Matrix Reasoning subtest ($r(63) = 0.26$, 95% CI: 0.02 , 0.48 , $p = 0.034$; Fig. 2B), along with the standard score from the Perceptual Reasoning Index (PRI) Composite ($r(63) = 0.34$, 95% CI: 0.11 , 0.54 , $p = 0.005$; Fig. 2C). Note that all WASI-II correlational analyses with task accuracy and zBMI survived at $p < 0.05$ following FDR correction. Finally, higher zBMI was associated with poorer performance on the Block Design subtest ($r(64) = -0.32$, 95% CI: -0.52 , -0.08 , $p = 0.010$; Fig. 2D).

Neural oscillatory responses

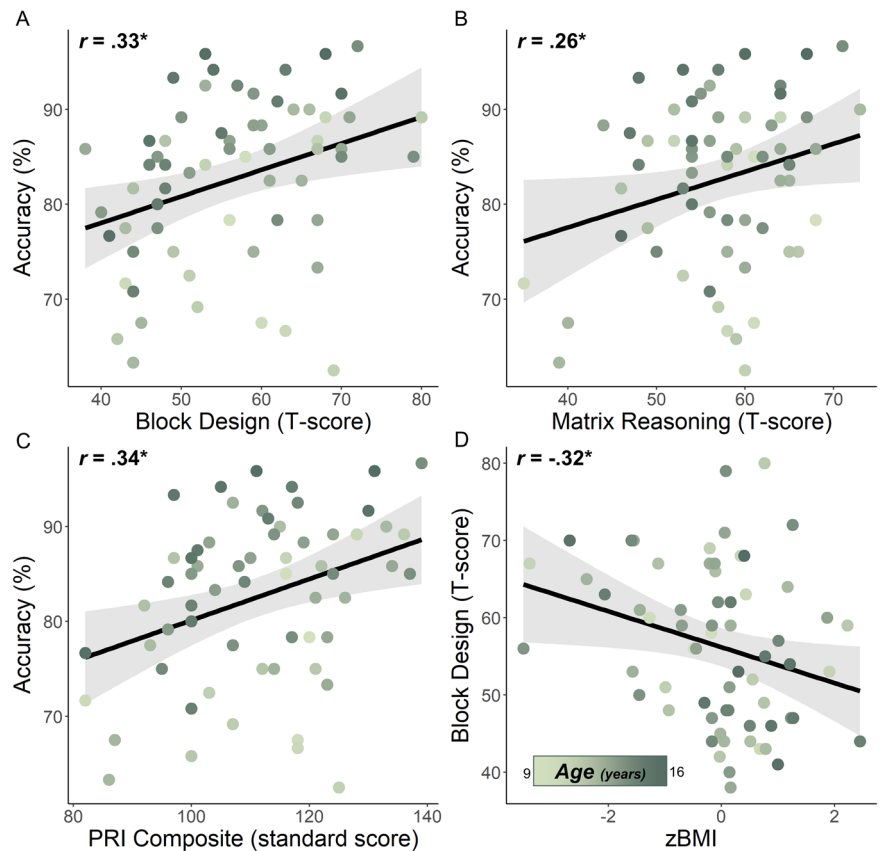
Sensor-level MEG data were transformed into the time-frequency domain and statistically examined using a rigorous two-stage approach. We observed robust neural oscillatory responses in three temporally and spectrally defined windows during the abstract reasoning task (Fig. 3). These included statistically significant theta oscillations (100–425 ms, 4–8 Hz, with an increase in power relative to the baseline period), robust and temporally extended alpha/beta oscillations (450–1450 ms, 8–16 Hz, with a decrease in power relative to the baseline), and gamma oscillations (200–1200 ms, 62–66 Hz, with an increase in power relative to baseline). Please refer to

Supplementary Fig. 1 for a map of the MEG sensor array showing the locations of the MEG gradiometers used to display the significant oscillatory responses. All responses were significant at $p < 0.005$ following multiple comparisons correction using nonparametric permutation testing. These time-frequency windows were imaged using a beamformer and one-sample t -tests were conducted per oscillatory response to assess the significant task-related responses serving abstract reasoning. These analyses revealed that significant oscillatory theta, alpha/beta, and gamma responses were widespread and extended across bilateral occipital, parietal, temporal, and frontal regions (Fig. 3; all $ps < 0.001$).

Whole-brain correlations with zBMI

To address our primary hypotheses, we standardized BMI scores for differences in sex and age (in months) based on the CDC growth charts according to Cole's LMS method^{71,72}. We then assessed the relationship between zBMI and theta, alpha/beta, and gamma oscillatory responses using voxel-wise correlations with the participant-level functional MEG images. Whole-brain correlations revealed that higher zBMI were associated with weaker theta oscillations within the left DLPFC ($r(57) = -0.46$, 95% CI: -0.64 , -0.23 , $p < 0.001$, corrected; Fig. 4) and the left TPJ ($r(57) = -0.41$, 95% CI: -0.60 , -0.17 , $p = 0.001$, corrected; Fig. 5A) during the abstract reasoning task. Interestingly, weaker theta oscillations in the left TPJ were also associated with worse performance on the abstract reasoning task (i.e., slower reaction times; $r(57) = -0.31$, 95% CI: -0.53 , -0.06 , $p = 0.016$; Fig. 5B). Theta activity in the left DLPFC and left TPJ were not significantly

Fig. 2 | Accuracy on the MEG abstract reasoning task was associated with measures of fluid intelligence. Accuracy (% correct) was significantly associated with scales from the Wechsler Abbreviated Scale of Intelligence – 2nd Edition (WASI-II), including the (A) Block Design and (B) Matrix Reasoning subtests, as well as the (C) Perceptual Reasoning Index (PRI) Composite. (D) Finally, zBMI was significantly associated with Block Design T-scores. The gray shaded area depicts the standard error of the mean. The gradient of the data points reflects each participant's age in years. Note that one participant had incomplete data for the Matrix Reasoning subtest and the PRI Composite ($n = 65$), but all participants had complete data for the Block Design subtest ($n = 66$). $*p < 0.05$.



associated with accuracy during the abstract reasoning task. No significant relationships were observed between zBMI and alpha/beta or gamma oscillations in these whole-brain analyses.

Exploratory relationships with dynamic functional connectivity

We conducted an exploratory analysis to determine whether theta-range dynamic functional connectivity among the left TPJ and DLPFC nodes was related to zBMI. Briefly, we computed the phase locking value (PLV)⁷³ between peak voxels in the left DLPFC and TPJ, averaged these across the active period for theta oscillations (i.e., the time window used in the beamforming analyses; Fig. 6A), and then normalized this mean active period value by the mean PLV during the pre-stimulus baseline period per participant. We then tested the association between PLV, zBMI, accuracy, and reaction time and found that higher zBMI was associated with weaker theta-range functional connectivity (i.e., PLV) between the left DLPFC and left TPJ, controlling for source power ($r(57) = -0.28$, 95% CI: $-0.50, -0.02$, $p = 0.035$; Fig. 6B). In addition, stronger PLV was associated with better performance on the abstract reasoning task in terms of accuracy ($r(57) = 0.38$, 95% CI: $0.14, 0.58$, $p = 0.003$; Fig. 6C) and reaction time ($r(57) = -0.34$, 95% CI: $-0.55, -0.09$, $p = 0.009$). Of note, as a sanity check, we also baseline-corrected the mean PLV during the active period by subtracting the mean PLV during the baseline period⁷⁴ and the results (i.e., correlations with zBMI and behavior) were very similar to the original analysis.

Discussion

In this study, we used an abstract reasoning task during high-density MEG recording in conjunction with age- and sex-adjusted BMI measures (i.e., zBMI) to examine whether the neural oscillatory dynamics underlying task performance scale with biometric measures. Briefly, abstract reasoning, which is tightly coupled with Gf and working memory, is known to undergo considerable development into early adulthood and is predictive of academic achievement^{41,42,45–47}. Obesity is known to negatively affect executive

function and higher order cognition^{29–31,49,50}, though its specific effects on the neural oscillatory dynamics underlying abstract reasoning have not previously been investigated in youth. This leaves a notable gap in the literature, as higher-order cognitive deficits associated with obesity have been widely demonstrated in the behavioral literature, yet the relationship between zBMI and the neural populations serving these cognitive processes remains unclear. Our key findings demonstrate that youth with greater zBMI had reduced theta oscillations in frontoparietal cortices and altered theta-frequency functional connectivity between these frontoparietal regions, with both oscillatory amplitude and connectivity scaling with task performance. Additionally, task accuracy and zBMI were significantly associated with gold-standard measures of Gf and abstract reasoning. These findings and their implications are discussed below.

Gf relies on the coordinated efforts across a network of regions and cognitive domains spanning the parietal and frontal cortices. Jung and Haier's P-FIT model postulates that sensory inputs to the parietal cortex are responsible for structural symbolism and abstraction, while interactions with the frontal cortex give rise to problem solving⁵². Several M/EEG studies have demonstrated spectrally-specific ensembles of coordinated oscillatory activity supporting Gf in fronto-parietal cortices^{47,75–77}. Further, the left DLPFC and TPJ have been reliably implicated in the P-FIT model, with a number of fMRI and PET studies reporting increased activation in these areas during tasks linked to Gf, such as figural and matrix reasoning tasks^{78,79}. Our findings linking the DLPFC and TPJ to abstract reasoning processes not only substantiate the existing literature, but also demonstrate the key roles of these regions and, importantly, their potential vulnerability to deviations from normal body mass, as we found that higher zBMI values scaled with altered theta oscillations in both regions. The TPJ is an important region for attentional control, as it is critically involved in the integration of salient contextual information, and it is modulated by the prefrontal cortex^{80,81}. Indeed, this process is essential to Gf more broadly, and matrix reasoning tasks in particular, whereby one must identify whether an image completes the rest of a pattern. Furthermore, we identified a direct

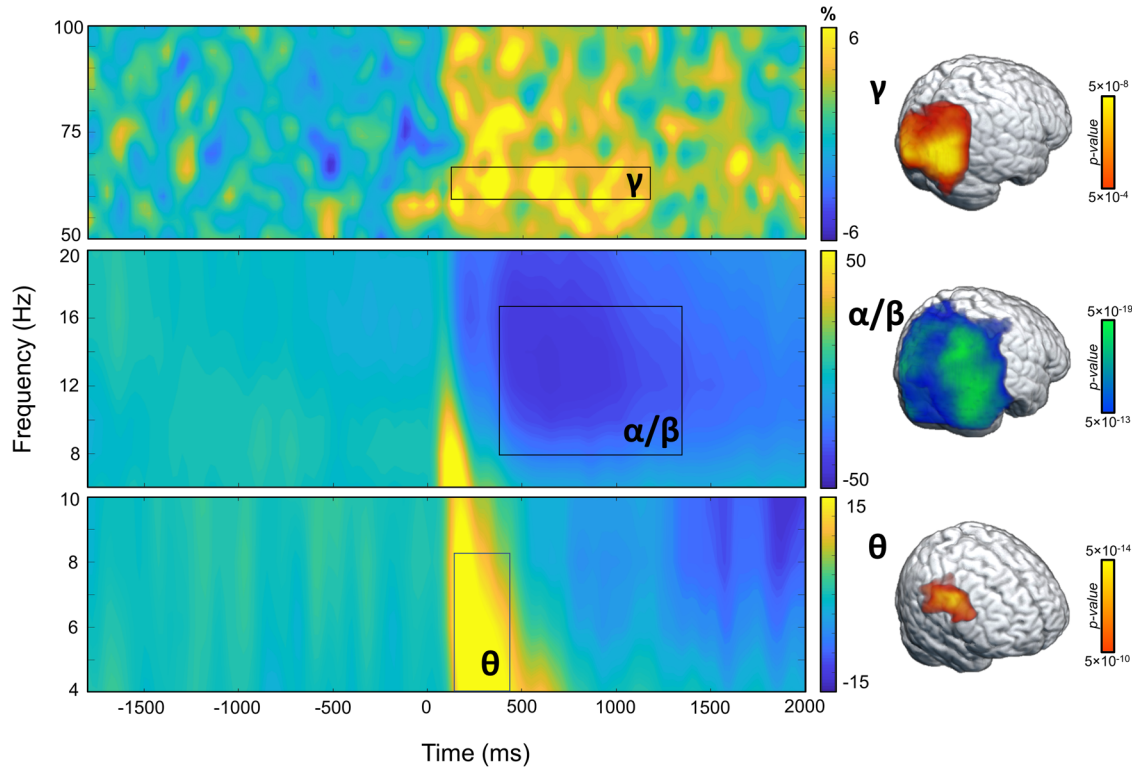


Fig. 3 | Neural oscillatory responses to the abstract reasoning task. (Left): Grand-averaged time-frequency spectrograms of MEG sensors exhibiting one or more significant oscillatory responses. Shown from top to bottom: gamma (62–66 Hz, 200–1200 ms; MEG1913), alpha/beta (8–16 Hz, 450–1450 ms; MEG2042), and theta (4–8 Hz, 100–425 ms; MEG1123). Each spectrogram displays frequency (Hz) on the y-axis and time (ms) on the x-axis. Signal power data are expressed as a percent

difference from the baseline period (–1800 to –800 ms) with color scale bars shown to the right of each spectrogram. Data from all 66 participants included for further analysis are represented in the spectrograms. Please refer to Supplementary Fig. 1 for a map of the MEG sensor locations. (Right): One-sample *t*-tests across all participants for each time-frequency component depicting the significant oscillatory responses serving abstract reasoning. Color scale bars display uncorrected *p* values.

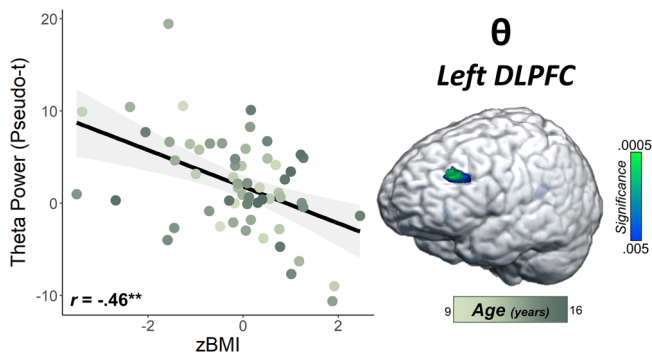


Fig. 4 | Higher zBMI is associated with blunted theta oscillations in the left DLPFC. (Left): Extracted pseudo-*t* values from the peak voxel in the left dorso-lateral prefrontal cortex (DLPFC) are plotted to show the significant relationship between zBMI (*x*-axis) and oscillatory theta power (pseudo-*t*, *y*-axis) during task performance. Note that data from 59 participants were used for analyses following outlier exclusion at the whole-brain level. The gray shaded area depicts the standard error of the mean. The gradient of the data points reflects each participant’s age in years, which was not significantly related to these findings. (Right): Thresholded correlation map across all participants showing the left DLPFC cluster where theta oscillations were inversely linked to zBMI. ***p* < 0.005.

link between weaker theta power and behavior in the TPJ, such that blunted theta activity was associated with slower response times. This may be due in part to the TPJ’s role in attending to salient stimuli and reorienting attention⁸², but could also be related to the intricate oscillatory dynamics supporting the higher-order processes associated with *Gf*. Finally, these results are in agreement with the pediatric obesity literature, including a

study from Kamijo et al. which found that children with obesity exhibited slower reaction times during trials requiring greater cognitive control (e.g., the incongruent condition of the Flanker task)^{83–87}.

The results of our exploratory functional connectivity analyses revealed that stronger theta-band connectivity between the DLPFC and TPJ was associated with better task performance, whereas higher zBMI was associated with weaker theta connectivity. Much of the functional connectivity literature is in the context of resting-state activity with most studies reporting disrupted connectivity in individuals with obesity⁸⁸. Recent studies using large-scale resting state datasets found that in adolescents, zBMI was negatively correlated with functional connectivity within- and between-functional networks¹⁶, and that BMI was positively associated with functional connectivity variability in the reward system in adults⁸⁹. The relationship between increased zBMI and weaker functional connectivity observed during the abstract reasoning task appears to be maladaptive, as individuals with stronger connectivity tended to perform better on the task.

Broadly, neural oscillations play an essential role in cognition, with theta, alpha, and gamma oscillations giving rise to cognitive processes important for *Gf* and abstract reasoning. For example, stronger decreases in alpha power relative to baseline (i.e., desynchronizations) have been associated with the allocation of attentional resources^{47,62,63}. Similarly, increases in gamma power have also been implicated in supporting top-down attentional control and higher-order cognition^{90,91}. Further, theta activity has been shown to be crucial in coordinating a wide range of cognitive processes, including selective attention⁶⁵, working memory^{92,93}, and fluid intelligence. For example, Riddle et al.⁹⁴ found that frontal theta activity became stronger with greater task demands, such as larger set sizes in a hierarchical cognitive control task⁹⁴, and others have found that greater cognitive demands during working memory tasks scale with oscillatory theta power^{95,96}. Alterations in theta oscillations and subsequent behavioral

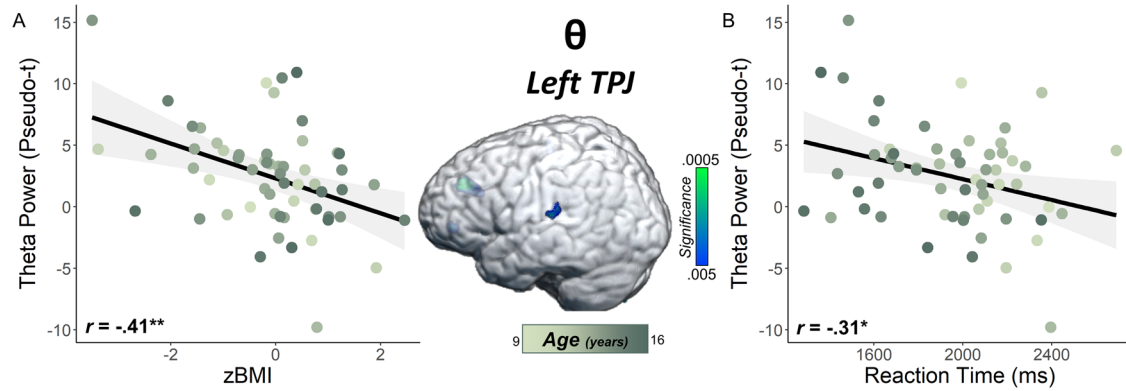


Fig. 5 | Elevated zBMI is associated with attenuated theta oscillations in the left TPJ. **A** Extracted pseudo-*t* values from the peak voxel in the left temporoparietal junction (TPJ) region are plotted to demonstrate the significant relationship between zBMI (*x*-axis) and weaker oscillatory theta power (pseudo-*t*, *y*-axis) during abstract reasoning. **B** Weaker oscillatory theta power in the left TPJ was associated with

slower reaction times (ms) during the abstract reasoning task. Note that data from 59 participants were used for analyses following outlier exclusion at the whole-brain level. In both scatterplots, the gray shaded area depicts the standard error of the mean. The gradient of the data points reflects each participant's age in years, which was not related to either finding. **p* < 0.05, ***p* < 0.005.

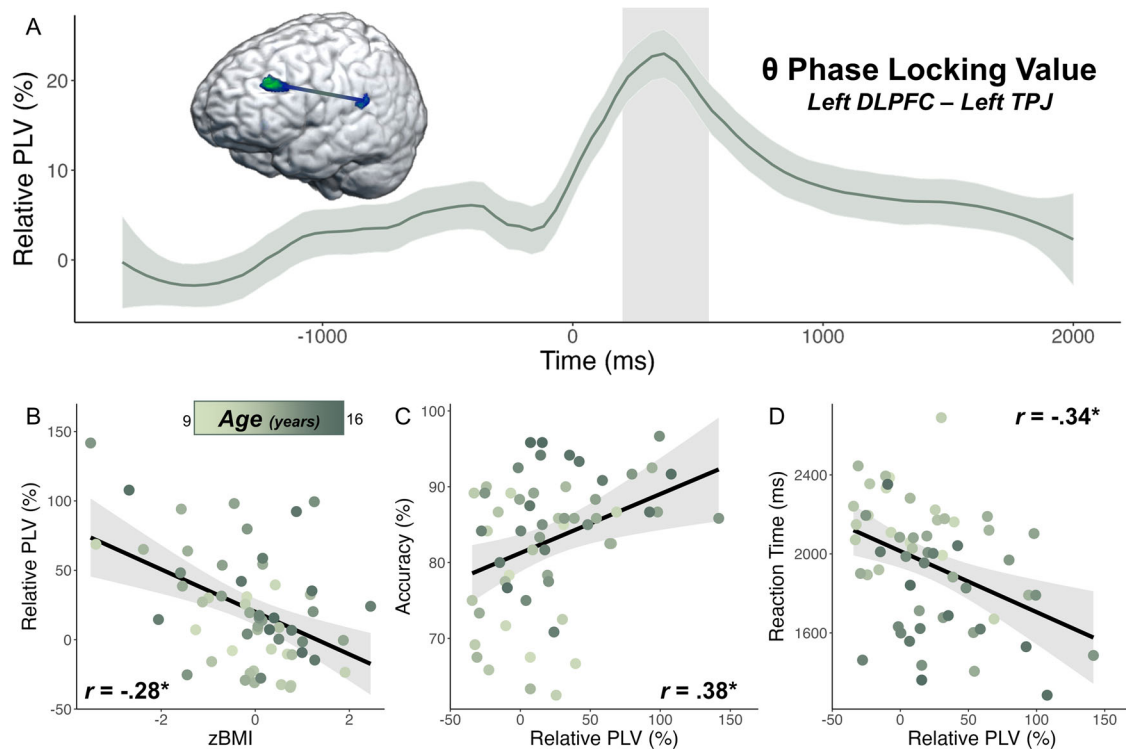


Fig. 6 | Exploratory analyses evaluating relationships between dynamic functional connectivity along the left DLPFC and left TPJ pathway with zBMI and task behavior. **A** The theta phase locking value (PLV) expressed as percent change relative to baseline was computed as a measure of dynamic functional connectivity between the left dorsolateral prefrontal cortex (DLPFC) and temporoparietal junction (TPJ). The gray shaded area depicts the active period (i.e., 100–425 ms), and the green shaded area depicts the standard error of the mean. Controlling for source

power, **(B)** higher zBMI was associated with weaker theta connectivity (i.e., hypo-connectivity) between the left DLPFC and left TPJ, while stronger theta PLVs scaled with better task performance in terms of **(C)** accuracy (% correct) and **(D)** reaction time (ms). Note that data from 59 participants were used for analyses after controlling for source power. The gray shaded areas depict the standard error of the mean. The gradient of the data points reflects each participant's age in years. **p* < 0.05, ***p* < 0.005.

deficits in working memory performance have also been reported in individuals with autism and schizophrenia^{97,98}, and prior work in our laboratory has demonstrated similar relationships between psychosocial distress and theta activity and behavior in youth performing the Flanker task⁹⁹, suggesting that these population-level neural dynamics may be critical to mental health function. Our finding that zBMI values are closely associated with the amplitude of theta oscillations may reflect selective perturbation of functioning in these networks due to health-related alterations in neurotransmitter cycling, mitochondrial perturbations, elevated inflammatory

levels, and/or related factors^{100–103}. However, additional work is needed to decipher the mechanisms and potential pathways involved in the context of obesity-related disease processes.

Before closing, it is important to acknowledge limitations of this study. First, though BMI is an accessible and easy metric to acquire and screen for obesity, using it as a measure of obesity in youth is less than ideal as it cannot account for the body's rapid growth and development during childhood and adolescence. Therefore, we used age- and sex-adjusted BMI (zBMI) to account for these differences in physical development. Unfortunately,

neither BMI nor zBMI distinguish between adipose and lean body mass, and thus, future investigations should consider utilizing more reliable or direct measures of obesity such as DEXA scans or hip-to-waist circumference ratios. Further, though the sample included individuals with overweight and obesity, the parent study (Dev-CoG)¹⁰⁴ did not target recruitment efforts to include individuals in this population, and thus, we were not sufficiently powered to separate our sample into groups for group-wise statistical analyses. Future studies that specifically target this population would benefit from being able to create several discrete groups based on obesity status for analysis (e.g., youth with healthy weight, youth with overweight, youth with obesity). Finally, we were unable to take pubertal status into account, and thus, future studies should evaluate the complex relationship between puberty and obesity on the neural dynamics serving higher-order cognitive processing.

Despite these limitations, our findings strongly suggest that normalized measurements of body mass scale with altered neural activity in regions serving *Gf*. Based on these findings and the extant literature, we hypothesize that studies that recruit participants with medically diagnosed obesity will observe even more robust relationships between obesity and neural indices supporting higher-order cognition. Our findings underscore the importance of research in this understudied, yet growing literature focused on youth with obesity, and the corresponding clinical implications during this crucial stage of cognitive development. Although a recently published study concluded that a domain-general cognitive control intervention had no significant effect on brain or behavioral outcomes in healthy children¹⁰⁵, a handful of studies in the behavioral literature have shown that interventions focused on improving attentional and cognitive control in youth with obesity can have positive effects^{106,107}. This may suggest that interventions aimed at improving abstract reasoning and *Gf* in youth who either have, or are at risk for developing obesity may be more efficacious in improving physical and cognitive outcomes for these individuals than for youth with healthy weight. However, more research will be needed to substantiate this claim. As rates of pediatric obesity continue to rise, understanding its long-term impacts on cognition is warranted. Coordinated efforts on all fronts are necessary for identifying and targeting efficacious treatments, and extensive work is needed to inform public policy and implement effective preventive strategies to reduce the individual and societal burdens of obesity.

Methods

Participants

Seventy-two youth between the ages of 9–16 years (Mean age = 13.09 years, SD = 1.93; See Table 1 and Supplementary Table 1 for full demographics) completed an abstract reasoning task as part of the National Science Foundation (NSF)-funded Developmental Chronnecto-Genomics (Dev-CoG) study¹⁰⁴. Note that the MEG data from this study have been previously published in a study evaluating developmental sex differences in the neural oscillatory dynamics serving abstract reasoning⁷⁵. Participants were recruited from the local community through advertisements, posted flyers, and community events. Flyers were also distributed through local elementary and middle schools. The racial and ethnic distribution of participants was monitored to ensure they reflected the demographics of the surrounding metropolitan area. Exclusionary criteria for enrollment in the study included any medical illness affecting CNS function, diagnosed neurological or psychiatric disorder, history of head trauma, current substance use, any medication known to affect CNS function, and the standard exclusionary criteria for MEG acquisition (e.g., dental braces, battery operated implants, and/or any type of ferromagnetic implanted material). Parents/guardians of participants signed informed consent forms, and the child and adolescent participants signed assent forms before proceeding with the study. All procedures were approved by the University of Nebraska Medical Center Institutional Review Board and all ethical regulations relevant to human research participants were followed in accordance with the Declaration of Helsinki.

Standardized Body Mass Index (zBMI)

Each participant's height and weight were measured at their study visit and used to create a BMI score. In the United States, weight status is defined by four classes based on BMI. Briefly, BMIs < 18.5 are classified as underweight, 18.5 to 24.9 are healthy weight, 25.0 to 29.9 are overweight, and 30.0 and above are classified as obesity. BMI scores were then standardized based on sex and age (in months) based on the CDC growth charts, which contain 10 smoothed percentiles (between the third and 97th) of BMI for children and adolescents between the ages of 24–240 months (~20 years) of age^{108,109}. These estimates were subsequently used to derive lambda (L , the power transformation to achieve normality), mu (M , mean or median), and sigma (S , coefficient of variation) parameters. The LMS parameters for BMI were derived from equations for smoothed percentiles^{109,110} based on Cole's LMS method^{71,72}. Estimates of these three parameters allow the BMI of youth to be expressed as a z-score (zBMI) and percentile relative to children of the same sex and age in the CDC growth charts using the following equation: $zBMI = [(BMI/M)^L - 1] \div (L \times S)$. Higher zBMI values were indicative of higher age- and sex-adjusted BMIs.

MEG and MRI data acquisition and analysis

Functional MEG data were collected using a MEGIN MEG system (Helsinki, Finland) equipped with 306 sensors (204 planar gradiometers, 102 magnetometers) using a 1 kHz sampling rate and an acquisition bandwidth of 0.1–330 Hz in a one-layer magnetically shielded room with active shielding engaged. During MEG recording, participants completed a non-progressive abstract reasoning task adapted from Raven's Progressive Matrices¹¹¹. MEG and MRI data processing closely followed previously reported pipelines^{47,60,61,70,75,76}. The structural MRI data were aligned parallel to the anterior and posterior commissures and transformed into standardized space. MEG data were subjected to environmental noise reduction and corrected for head motion¹¹². Only data from the 204 planar gradiometers were used for further analysis. All MEG and MRI data were further processed in BESA (Research: Version 7.1; MRI: Version 3.0; Statistics: Version 2.1). Cardiac and ocular artifacts were removed from the MEG data using signal space projection¹¹³, and this correction was accounted for during source reconstruction. The data were separated into 6500 ms epochs. Only trials with correct responses were considered for further analysis. Epochs containing artifacts were rejected using a fixed threshold method that was set per participant and supplemented with visual inspection. Briefly, in MEG, the raw signal amplitude is strongly affected by the distance between the brain and the MEG sensor array, as the magnetic field strength falls off sharply as the distance from the current source (i.e., brain) increases. To account for this source of variance across participants, as well as other sources of variance, we used an individualized threshold based on the signal distribution for both amplitude and gradient to reject artifacts. The average amplitude threshold across all participants was 1361.72 (SD = 352.63) fT/cm, the average gradient threshold was 283.98 (SD = 125.99) fT/(cm*ms), and an average of 86.19 (SD = 11.80) trials out of the original 120 were used for further analysis. The number of trials included in the final MEG analyses was not significantly associated with zBMI ($r = -0.17$, $p = 0.187$) or age ($r = 0.21$, $p = 0.118$). We then transformed the artifact-free epochs into the time-frequency domain (resolution: 2 Hz, 25 ms)^{114,115} and these were normalized by the baseline power of each respective bin, calculated as the mean power from –1800 to –800 ms, relative to stimulus onset.

Statistics and reproducibility

The time-frequency windows for subsequent source imaging were identified using a stringent two-stage statistical approach that utilized paired-sample *t*-tests against baseline on each pixel in the spectrogram (per sensor) at the first stage, followed up with cluster-based nonparametric permutation testing at the second level. This testing was conducted across all participants and the entire frequency range (4–100 Hz) and used an initial cluster threshold of a two-tailed $p < 0.05$ and 5000 permutations. These methods are described in

depth in our recent publications^{116,117}. Time-frequency resolved source images were computed using the dynamic imaging of coherent sources (DICS) beamformer to image oscillatory activity in the time-frequency windows of interest per participant^{118–120}. Following convention, we used task and baseline periods of equal duration and bandwidth for each time-frequency cluster identified in the sensor-level analysis to derive noise-normalized source power estimates per voxel (resolution: $4 \times 4 \times 4$ mm) for each participant. These maps reflect power differences between the active and baseline periods and were transformed into standardized space using the same transform that was applied to the native space structural images per participant and then spatially resampled. To examine oscillatory activity specific to abstract reasoning, source images for each participant were included in whole-brain one-sample *t*-tests per time-frequency window to identify significant neural oscillatory responses serving abstract reasoning.

To probe whole-brain associations between neural oscillatory power serving abstract reasoning and zBMI, we computed voxel-wise correlations between zBMI and each neural oscillatory map (i.e., theta, alpha/beta, gamma)^{75,121,122}. Individual participant-level maps containing significant artifacts were excluded from further analysis. To aid in interpretation, pseudo-*t* values were extracted from the peak voxel of each significant cluster per participant and plotted. To account for multiple comparisons, a two-tailed significance threshold of $p < 0.005$ was used for the identification of significant clusters in all whole-brain statistical maps, accompanied by a cluster (*k*) threshold of at least 12 contiguous voxels (i.e., >750 mm³ of brain tissue) based on the theory of Gaussian random fields^{123–125}. All whole-brain statistical analyses were computed using a custom function in MATLAB v.R2018b (MathWorks; Natick, Massachusetts) and other statistical analyses were conducted in IBM SPSS v.29.

Exploratory functional connectivity analyses

We then conducted exploratory dynamic functional connectivity analyses between the significant cortical regions derived from the whole-brain correlation maps identified in our main analyses. Phase locking was computed within the same time-frequency windows derived from our sensor-level statistical analyses. Specifically, we estimated the phase locking value (PLV)⁷³ between the significant clusters identified through the correlation maps. The PLV reflects the intertrial variability of the phase relationship between pairs of brain regions as a function of time. Values close to one indicate strong synchronicity (i.e., phase locking) between the two brain regions within the specific time window across trials, whereas values close to zero indicate substantial phase variation between the two signals and, thus, weak synchronicity (connectivity) between the two regions. We extracted the mean PLV relative to the baseline period (expressed as a percent change from baseline) per participant within the time-frequency windows used for beamforming, which we then correlated with zBMI and measures of task performance (i.e., accuracy, reaction time), controlling for source power⁹⁹. Of note, as a sanity check, we also baseline-corrected the mean PLV by subtracting the mean PLV during the baseline period⁷⁴, which we then correlated with zBMI and task performance, controlling for source power. The results were very similar, so we report only the analyses that used the normalization approach, with PLV expressed as percent change from baseline.

Reporting summary

Further information on research design is available in the Nature Portfolio Reporting Summary linked to this article.

Data availability

De-identified MEG and MRI data have been made available to the public through the Collaborative Informatics and Neuroimaging Suite (COINS; <https://coins.trendcenter.org>) database. The data pertaining to this study are under the Dev-CoG ID for the Omaha site (“DEVCOGB”). Demographic and other assessment data for this study is also available through COINS. Requests for additional data can be fulfilled via the corresponding author on reasonable request.

Code availability

The MEG and MRI analyses reported herein utilized the Brain Electrical Source Analysis software (BESA Research: version 7.1; BESA MRI: version 3.0; BESA Statistics: version 2.1). We also used Matlab version R2018b and IBM SPSS version 29 for some statistical analyses. Any requests for code or batch functions used in these analyses can be fulfilled via the corresponding author upon reasonable request.

Received: 29 November 2023; Accepted: 18 September 2024;

Published online: 09 October 2024

References

- World Health Organization. Noncommunicable diseases: Childhood overweight and obesity. <https://www.who.int/news-room/questions-and-answers/item/noncommunicable-diseases-childhood-overweight-and-obesity> (2020).
- Fryar, C. D., Carroll, M. D. & Afful, J. Prevalence of overweight, obesity, and severe obesity among children and adolescents aged 2–19 years: United States, 1963–1965 through 2017–2018. *NCHS Health E-Stats*. <https://www.cdc.gov/nchs/data/hestat/obesity-child-17-18/obesity-child.htm> (2020).
- Stierman, B. et al. National Health and Nutrition Examination Survey 2017–March 2020 Prepandemic Data Files Development of Files and Prevalence Estimates for Selected Health Outcomes. *Natl Health Stat. Rep.* **158**, 1–20 (2021).
- Palmer, M. K. & Toth, P. P. Trends in lipids, obesity, metabolic syndrome, and diabetes mellitus in the United States: An NHANES Analysis (2003–2004 to 2013–2014). *Obesity* **27**, 309–314 (2019).
- Kopelman, P. G. Obesity as a medical problem. *Nature* **404**, 635–643 (2000).
- Fontaine, K. R., Redden, D. T., Wang, C., Westfall, A. O. & Allison, D. B. Years of life lost due to obesity. *JAMA* **289**, 187–193 (2003).
- Mandviwala, T., Khalid, U. & Deswal, A. Obesity and cardiovascular disease: a risk factor or a risk marker? *Curr. Atheroscler. Rep.* **18**, 21 (2016).
- Poirier, P. et al. Obesity and cardiovascular disease: pathophysiology, evaluation, and effect of weight loss. *Circulation* **113**, 898–918 (2006).
- Rippe, J. M., Crossley, S. & Ringer, R. Obesity as a chronic disease: modern medical and lifestyle management. *J. Am. Diet. Assoc.* **98**, S9–S15 (1998).
- Pi-Sunyer, X. The medical risks of obesity. *Postgrad. Med.* **121**, 21–33 (2009).
- Laurent, J. S. et al. Associations among body mass index, cortical thickness, and executive function in children. *JAMA Pediatr.* **174**, 170–177 (2020).
- Ronan, L., Alexander-Bloch, A. & Fletcher, P. C. Childhood obesity, cortical structure, and executive function in healthy children. *Cereb. Cortex* **30**, 2519–2528 (2020).
- Saute, R. L., Soder, R. B., Alves Filho, J. O., Baldisserotto, M. & Franco, A. R. Increased brain cortical thickness associated with visceral fat in adolescents. *Pediatr. Obes.* **13**, 74–77 (2018).
- Sharkey, R. J., Karama, S. & Dagher, A. Overweight is not associated with cortical thickness alterations in children. *Front. Neurosci.* **9**, 24 (2015).
- Yau, P. L., Kang, E. H., Javier, D. C. & Convit, A. Preliminary evidence of cognitive and brain abnormalities in uncomplicated adolescent obesity. *Obesity* **22**, 1865–1871 (2014).
- Kaltenhauser, S. et al. Association of body mass index and waist circumference with imaging metrics of brain integrity and functional connectivity in children aged 9 to 10 years in the US, 2016–2018. *JAMA Netw. Open* **6**, e2314193 (2023).
- Frith, C. & Dolan, R. The role of the prefrontal cortex in higher cognitive functions. *Brain Res. Cognit. Brain Res.* **5**, 175–181 (1996).

18. Arain, M. et al. Maturation of the adolescent brain. *Neuropsychiatr. Dis. Treat.* **9**, 449–461 (2013).
19. Fuster, J. M. Prefrontal neurons in networks of executive memory. *Brain Res. Bull.* **52**, 331–336 (2000).
20. Mezzacappa, E. Executive Function. in *Reference Module in Neuroscience and Biobehavioral Psychology* <https://doi.org/10.1016/B978-0-12-809324-5.06001-6> (Elsevier, 2017).
21. Luna, B., Marek, S., Larsen, B., Tervo-Clemmens, B. & Chahal, R. An integrative model of the maturation of cognitive control. *Annu. Rev. Neurosci.* **38**, 151–170 (2015).
22. Doebel, S. Rethinking executive function and its development. *Perspect. Psychol. Sci.* **15**, 942–956 (2020).
23. Ferguson, H. J., Brunson, V. E. A. & Bradford, E. E. F. The developmental trajectories of executive function from adolescence to old age. *Sci. Rep.* **11**, 1382 (2021).
24. Garon, N., Bryson, S. E. & Smith, I. M. Executive function in preschoolers: a review using an integrative framework. *Psychol. Bull.* **134**, 31–60 (2008).
25. Lentoor, A. G. Obesity and neurocognitive performance of memory, attention, and executive function. *NeuroSci* **3**, 376–386 (2022).
26. Sánchez-SanSegundo, M. et al. The role of BMI, body fat mass and visceral fat in executive function in individuals with overweight and obesity. *Nutrients* **13**, 2259 (2021).
27. Fergenbaum, J. H. et al. Obesity and lowered cognitive performance in a Canadian First Nations population. *Obesity* **17**, 1957–1963 (2009).
28. Gunstad, J. et al. Elevated body mass index is associated with executive dysfunction in otherwise healthy adults. *Compr. Psychiatry* **48**, 57–61 (2007).
29. Christina, S. D., Sangeetha, A., Kumaresan, M., Varadharaju, B. & Hemachandrika, C. Association between Working Memory and Obesity among Secondary School Children. *J. Pharm. Res. Int.* **79–84** <https://doi.org/10.9734/jpri/2021/v33i29B31592> (2021).
30. Francis, L. A. & Susman, E. J. Self-regulation and rapid weight gain in children from age 3 to 12 years. *Arch. Pediatr. Adolesc. Med.* **163**, 297–302 (2009).
31. Reinert, K. R. S., Po'e, E. K. & Barkin, S. L. The relationship between executive function and obesity in children and adolescents: a systematic literature review. *J. Obes.* **2013**, 1–10 (2013).
32. Mamrot, P. & Hanć, T. The association of the executive functions with overweight and obesity indicators in children and adolescents: a literature review. *Neurosci. Biobehav. Rev.* **107**, 59–68 (2019).
33. Yang, Y., Shields, G. S., Guo, C. & Liu, Y. Executive function performance in obesity and overweight individuals: a meta-analysis and review. *Neurosci. Biobehav. Rev.* **84**, 225–244 (2018).
34. Alarcón, G., Ray, S. & Nagel, B. J. Lower working memory performance in overweight and obese adolescents is mediated by white matter microstructure. *J. Int. Neuropsychol. Soc.* **22**, 281–292 (2016).
35. Wirt, T. et al. Associations between inhibitory control and body weight in German primary school children. *Eat. Behav.* **15**, 9–12 (2014).
36. Maayan, L., Hoogendoorn, C., Sweat, V. & Convit, A. Disinhibited eating in obese adolescents is associated with orbitofrontal volume reductions and executive dysfunction. *Obesity* **19**, 1382–1387 (2011).
37. O'Brien, P. D., Hinder, L. M., Callaghan, B. C. & Feldman, E. L. Neurological consequences of obesity. *Lancet Neurol.* **16**, 465–477 (2017).
38. Verdejo-García, A. et al. Selective alterations within executive functions in adolescents with excess weight. *Obesity* **18**, 1572–1578 (2010).
39. Hughes, S. O., Power, T. G., O'Connor, T. M. & Orlet Fisher, J. Executive functioning, emotion regulation, eating self-regulation, and weight status in low-income preschool children: how do they relate? *Appetite* **89**, 1–9 (2015).
40. Fitzpatrick, S., Gilbert, S. & Serpell, L. Systematic review: are overweight and obese individuals impaired on behavioural tasks of executive functioning? *Neuropsychol. Rev.* **23**, 138–156 (2013).
41. Conway, A. R. A., Cowan, N., Bunting, M. F., Theriault, D. J. & Minkoff, S. R. B. A latent variable analysis of working memory capacity, short-term memory capacity, processing speed, and general fluid intelligence. *Intelligence* **30**, 163–183 (2002).
42. Lulewicz, A. & Nęcka, E. Capacity, Control, or Both – Which Aspects of Working Memory Contribute to Children's General Fluid Intelligence? *Pol. Psychol. Bull.* **47** <https://doi.org/10.1515/ppb-2016-0003> (2016).
43. Cattell, R. B. Theory of fluid and crystallized intelligence: a critical experiment. *J. Educ. Psychol.* **54**, 1–22 (1963).
44. Schroeders, U., Schipolowski, S., Zettler, I., Golle, J. & Wilhelm, O. Do the smart get smarter? Development of fluid and crystallized intelligence in 3rd grade. *Intelligence* **59**, 84–95 (2016).
45. Gómez-Veiga, I., Vila Chaves, J. O., Duque, G. & García Madruga, J. A. A new look to a classic issue: reasoning and academic achievement at secondary school. *Front. Psychol.* **9**, 400 (2018).
46. Green, C. T., Bunge, S. A., Briones Chiongbian, V., Barrow, M. & Ferrer, E. Fluid reasoning predicts future mathematical performance among children and adolescents. *J. Exp. Child Psychol.* **157**, 125–143 (2017).
47. Taylor, B. K. et al. Longitudinal changes in the neural oscillatory dynamics underlying abstract reasoning in children and adolescents. *NeuroImage* **253**, 119094 (2022).
48. Raven, J. Raven progressive matrices. in *Handbook of Nonverbal Assessment* (ed. McCallum, R. S.) 223–237. https://doi.org/10.1007/978-1-4615-0153-4_11 (Springer, 2003).
49. Poh, B. K. et al. Low socioeconomic status and severe obesity are linked to poor cognitive performance in Malaysian children. *BMC Public Health* **19**, 541 (2019).
50. Klinedinst, B. S. et al. Aging-related changes in fluid intelligence, muscle and adipose mass, and sex-specific immunologic mediation: a longitudinal UK Biobank study. *Brain Behav. Immun.* **82**, 396–405 (2019).
51. Carlozzi, N. E. Kaufman brief intelligence test. in *Encyclopedia of Clinical Neuropsychology* (eds. Kreutzer, J. S., DeLuca, J. & Caplan, B.) 1398–1400. https://doi.org/10.1007/978-0-387-79948-3_1062 (Springer, 2011).
52. Jung, R. E. & Haier, R. J. The Parieto-Frontal Integration Theory (P-FIT) of intelligence: converging neuroimaging evidence. *Behav. Brain Sci.* **30**, 135–154 (2007).
53. Basten, U., Hilger, K. & Fiebach, C. J. Where smart brains are different: a quantitative meta-analysis of functional and structural brain imaging studies on intelligence. *Intelligence* **51**, 10–27 (2015).
54. Shaw, P. Intelligence and the developing human brain. *BioEssays* **29**, 962–973 (2007).
55. Prabhakaran, V., Smith, J. A. L., Desmond, J. E., Glover, G. H. & Gabrieli, J. D. E. Neural substrates of fluid reasoning: an fMRI study of neocortical activation during performance of the Raven's progressive matrices test. *Cognit. Psychol.* **33**, 43–63 (1997).
56. Owen, A. M., McMillan, K. M., Laird, A. R. & Bullmore, E. N-back working memory paradigm: a meta-analysis of normative functional neuroimaging studies. *Hum. Brain Mapp.* **25**, 46–59 (2005).
57. Lie, C.-H., Specht, K., Marshall, J. C. & Fink, G. R. Using fMRI to decompose the neural processes underlying the Wisconsin Card Sorting Test. *NeuroImage* **30**, 1038–1049 (2006).
58. Heinrichs-Graham, E. et al. Auditory experience modulates frontoparietal theta activity serving fluid intelligence. *Brain Commun.* **4**, fcac093 (2022).
59. Neubauer, A. C., Wammerl, M., Benedek, M., Jauk, E. & Jaušovec, N. The influence of transcranial alternating current stimulation (tACS)

- on fluid intelligence: an fMRI study. *Personal. Individ. Differ.* **118**, 50–55 (2017).
60. Schantell, M. et al. Stress and psychosocial distress scale with blunted oscillatory dynamics serving abstract reasoning. *Depress Anxiety* **2024**, e4720803 (2024).
 61. Penhale, S. H. et al. Healthy aging alters the oscillatory dynamics and fronto-parietal connectivity serving fluid intelligence. *Hum. Brain Mapp.* **45**, e26591 (2024).
 62. Koshy, S. M. et al. Numerical working memory alters alpha-beta oscillations and connectivity in the parietal cortices. *Hum. Brain Mapp.* **41**, 3709–3719 (2020).
 63. Stoll, F. M. et al. The effects of cognitive control and time on frontal beta oscillations. *Cereb. Cortex* **26**, 1715–1732 (2016).
 64. Cavanagh, J. F. & Frank, M. J. Frontal theta as a mechanism for cognitive control. *Trends Cognit. Sci.* **18**, 414–421 (2014).
 65. Son, J. J. et al. Oscillatory dynamics serving visual selective attention during a Simon task. *Brain Commun.* **5**, fcad131 (2023).
 66. McDermott, T. J. et al. Attention training improves aberrant neural dynamics during working memory processing in veterans with PTSD. *Cognit. Affect. Behav. Neurosci.* **16**, 1140–1149 (2016).
 67. Chung, S. Body mass index and body composition scaling to height in children and adolescent. *Ann. Pediatr. Endocrinol. Metab.* **20**, 125–129 (2015).
 68. Kuczumski, R. J. et al. CDC growth charts: United States. *Adv. Data.* **8**, 1–27 (2000).
 69. Hampl, S. E. et al. Clinical practice guideline for the evaluation and treatment of children and adolescents with obesity. *Pediatrics* **151**, e2022060640 (2023).
 70. Dietz, S. M. et al. Elevated CRP and TNF- α levels are associated with blunted neural oscillations serving fluid intelligence. *Brain Behav. Immun.* **114**, 430–437 (2023).
 71. Cole, T. J. & Green, P. J. Smoothing reference centile curves: the LMS method and penalized likelihood. *Stat. Med.* **11**, 1305–1319 (1992).
 72. Cole, T. J. The LMS method for constructing normalized growth standards. *Eur. J. Clin. Nutr.* **44**, 45–60 (1990).
 73. Lachaux, J. P., Rodriguez, E., Martinerie, J. & Varela, F. J. Measuring phase synchrony in brain signals. *Hum. Brain Mapp.* **8**, 194–208 (1999).
 74. Wiesman, A. I. et al. Quiet connections: reduced fronto-temporal connectivity in nondemented Parkinson's Disease during working memory encoding. *Hum. Brain Mapp.* **37**, 3224–3235 (2016).
 75. Taylor, B. K. et al. Neural oscillatory dynamics serving abstract reasoning reveal robust sex differences in typically-developing children and adolescents. *Dev. Cognit. Neurosci.* **42**, 100770 (2020).
 76. Arif, Y., Spooner, R. K., Heinrichs-Graham, E. & Wilson, T. W. High-definition transcranial direct current stimulation modulates performance and alpha/beta parieto-frontal connectivity serving fluid intelligence. *J. Physiol.* **599**, 5451–5463 (2021).
 77. Miasnikova, A., Perevoznyuk, G., Martynova, O. & Baklushev, M. Cross-frequency phase coupling of brain oscillations and relevance attribution as saliency detection in abstract reasoning. *Neurosci. Res.* **166**, 26–33 (2021).
 78. Wharton, C. M. et al. Toward neuroanatomical models of analogy: A positron emission tomography study of analogical mapping. *Cognit. Psychol.* **40**, 173–197 (2000).
 79. Hampshire, A., Thompson, R., Duncan, J. & Owen, A. M. Lateral prefrontal cortex subregions make dissociable contributions during fluid reasoning. *Cereb. Cortex* **21**, 1–10 (2011).
 80. DiQuattro, N. E. & Geng, J. J. Contextual knowledge configures attentional control networks. *J. Neurosci.* **31**, 18026–18035 (2011).
 81. Weidner, R., Krummenacher, J., Reimann, B., Müller, H. J. & Fink, G. R. Sources of top-down control in visual search. *J. Cognit. Neurosci.* **21**, 2100–2113 (2009).
 82. Corbetta, M., Patel, G. & Shulman, G. L. The reorienting system of the human brain: from environment to theory of mind. *Neuron* **58**, 306–324 (2008).
 83. Kamijo, K. et al. The negative association of childhood obesity to cognitive control of action monitoring. *Cereb. Cortex* **24**, 654–662 (2014).
 84. Spyridaki, E. C., Avgoustinaki, P. D. & Margioris, A. N. Obesity, inflammation and cognition. *Curr. Opin. Behav. Sci.* **9**, 169–175 (2016).
 85. Spyridaki, E. C. et al. The association between obesity and fluid intelligence impairment is mediated by chronic low-grade inflammation. *Br. J. Nutr.* **112**, 1724–1734 (2014).
 86. Gray, J. C., Schvey, N. A. & Tanofsky-Kraff, M. Demographic, psychological, behavioral, and cognitive correlates of BMI in youth: findings from the Adolescent Brain Cognitive Development (ABCD) study. *Psychol. Med.* **50**, 1539–1547 (2020).
 87. Cadenas-Sanchez, C. et al. Physical activity, sedentary time, and fitness in relation to brain shapes in children with overweight/obesity: Links to intelligence. *Scand. J. Med. Sci. Sports* **33**, 319–330 (2023).
 88. Syan, S. K. et al. Dysregulated resting state functional connectivity and obesity: a systematic review. *Neurosci. Biobehav. Rev.* **131**, 270–292 (2021).
 89. Guo, Y., Xia, Y. & Chen, K. The body mass index is associated with increased temporal variability of functional connectivity in brain reward system. *Front. Nutr.* **10**, 1210726 (2023).
 90. Jensen, O., Kaiser, J. & Lachaux, J.-P. Human gamma-frequency oscillations associated with attention and memory. *Trends Neurosci.* **30**, 317–324 (2007).
 91. Wiesman, A. I., Koshy, S. M., Heinrichs-Graham, E. & Wilson, T. W. Beta and Gamma oscillations index cognitive interference effects across a distributed motor network. *NeuroImage* **213**, 116747 (2020).
 92. Ratcliffe, O., Shapiro, K. & Staresina, B. P. Fronto-medial theta coordinates posterior maintenance of working memory content. *Curr. Biol.* **32**, 2121–2129.e3 (2022).
 93. Springer, S. D. et al. Age-related alterations in the oscillatory dynamics serving verbal working memory processing. *Aging* **15**, 14574–14590 (2023).
 94. Riddle, J., Vogelsang, D. A., Hwang, K., Cellier, D. & D'Esposito, M. Distinct oscillatory dynamics underlie different components of hierarchical cognitive control. *J. Neurosci.* **40**, 4945–4953 (2020).
 95. Jensen, O. & Tesche, C. D. Frontal theta activity in humans increases with memory load in a working memory task. *Eur. J. Neurosci.* **15**, 1395–1399 (2002).
 96. Proskovec, A. L., Heinrichs-Graham, E. & Wilson, T. W. Load modulates the alpha and beta oscillatory dynamics serving verbal working memory. *NeuroImage* **184**, 256–265 (2019).
 97. Larrain-Valenzuela, J. et al. Theta and Alpha oscillation impairments in autistic spectrum disorder reflect working memory deficit. *Sci. Rep.* **7**, 14328 (2017).
 98. Schmiecht, C., Brand, A., Hildebrandt, H. & Basar-Eroglu, C. Event-related theta oscillations during working memory tasks in patients with schizophrenia and healthy controls. *Cognit. Brain Res.* **25**, 936–947 (2005).
 99. Schantell, M. et al. Theta oscillatory dynamics serving cognitive control index psychosocial distress in youth. *Neurobiol. Stress* **29**, 100599 (2024).
 100. Spooner, R. K. et al. Clinical markers of HIV predict redox-regulated neural and behavioral function in the sensorimotor system. *Free Radic. Biol. Med.* **212**, 322–329 (2024).
 101. Spooner, R. K. et al. Mitochondrial redox environments predict sensorimotor brain-behavior dynamics in adults with HIV. *Brain Behav. Immun.* **107**, 265–275 (2023).

102. Spooner, R. K. et al. Neural oscillatory activity serving sensorimotor control is predicted by superoxide-sensitive mitochondrial redox environments. *Proc. Natl Acad. Sci. USA* **118**, e2104569118 (2021).
103. Spooner, R. K. et al. Neuroinflammatory profiles regulated by the redox environment predicted cognitive dysfunction in people living with HIV: A cross-sectional study. *EBioMedicine* **70**, 103487 (2021).
104. Stephen, J. M. et al. The Developmental Chronnecto-Genomics (Dev-CoG) study: a multimodal study on the developing brain. *NeuroImage* **225**, 117438 (2021).
105. Ganesan, K. et al. Cognitive control training with domain-general response inhibition does not change children's brains or behavior. *Nat. Neurosci.* **27**, 1364–1375 (2024).
106. Hayes, J. F., Eichen, D. M., Barch, D. M. & Wilfley, D. E. Executive function in childhood obesity: promising intervention strategies to optimize treatment outcomes. *Appetite* **124**, 10–23 (2018).
107. Verbeken, S., Braet, C., Goossens, L. & van der Oord, S. Executive function training with game elements for obese children: a novel treatment to enhance self-regulatory abilities for weight-control. *Behav. Res. Ther.* **51**, 290–299 (2013).
108. Freedman, D. S., Woo, J. G., Ogden, C. L., Xu, J. H. & Cole, T. J. Distance and percentage distance from median BMI as alternatives to BMI z score. *Br. J. Nutr.* **124**, 493–500 (2020).
109. Flegal, K. M. et al. Characterizing extreme values of body mass index-for-age by using the 2000 Centers for Disease Control and Prevention growth charts. *Am. J. Clin. Nutr.* **90**, 1314–1320 (2009).
110. Flegal, K. M. & Cole, T. J. Construction of LMS parameters for the centers for disease control and prevention 2000 growth charts. *Natl. Health Stat. Rep.* **11**, 1–3 (2013).
111. John & Raven, J. Raven Progressive Matrices. in *Handbook of Nonverbal Assessment* (ed. McCallum, R. S.) 223–237. https://doi.org/10.1007/978-1-4615-0153-4_11 (Springer, 2003).
112. Taulu, S. & Simola, J. Spatiotemporal signal space separation method for rejecting nearby interference in MEG measurements. *Phys. Med. Biol.* **51**, 1759–1768 (2006).
113. Uusitalo, M. A. & Ilmoniemi, R. J. Signal-space projection method for separating MEG or EEG into components. *Med. Biol. Eng. Comput.* **35**, 135–140 (1997).
114. Papp, N. & Ktonas, P. Critical evaluation of complex demodulation techniques for the quantification of bioelectrical activity. *Biomed. Sci. Instrum.* **13**, 135–145 (1977).
115. Kovach, C. K. & Gander, P. E. The demodulated band transform. *J. Neurosci. Methods* **261**, 135–154 (2016).
116. Wiesman, A. I. & Wilson, T. W. Attention modulates the gating of primary somatosensory oscillations. *NeuroImage* **211**, 116610 (2020).
117. Wiesman, A. I., Christopher-Hayes, N. J., Eastman, J. A., Heinrichs-Graham, E. & Wilson, T. W. Response certainty during bimanual movements reduces gamma oscillations in primary motor cortex. *NeuroImage* **224**, 117448 (2021).
118. Van Veen, B. D., van Drongelen, W., Yuchtman, M. & Suzuki, A. Localization of brain electrical activity via linearly constrained minimum variance spatial filtering. *IEEE Trans. Biomed. Eng.* **44**, 867–880 (1997).
119. Gross, J. et al. Dynamic imaging of coherent sources: Studying neural interactions in the human brain. *Proc. Natl Acad. Sci. USA* **98**, 694–699 (2001).
120. Dalal, S. S., Sekihara, K. & Nagarajan, S. S. Modified beamformers for coherent source region suppression. *IEEE Trans. Biomed. Eng.* **53**, 1357–1363 (2006).
121. Embury, C. M. et al. Neural dynamics of verbal working memory processing in children and adolescents. *NeuroImage* **185**, 191–197 (2019).
122. Groff, B. R. et al. Age-related visual dynamics in HIV-infected adults with cognitive impairment. *Neurol. Neuroimmunol. Neuroinflamm.* **7**, e690 (2020).
123. Poline, J. B., Worsley, K. J., Holmes, A. P., Frackowiak, R. S. & Friston, K. J. Estimating smoothness in statistical parametric maps: variability of p values. *J. Comput. Assist. Tomogr.* **19**, 788–796 (1995).
124. Worsley, K. J. et al. A unified statistical approach for determining significant signals in images of cerebral activation. *Hum. Brain Mapp.* **4**, 58–73 (1996).
125. Worsley, K. J., Andermann, M., Koulis, T., MacDonald, D. & Evans, A. C. Detecting changes in nonisotropic images. *Hum. Brain Mapp.* **8**, 98–101 (1999).

Acknowledgements

This research was supported by grants F31-DA056296 (Schantell), R01-MH121101 (Wilson), P20-GM144641 (Wilson, Heinrichs-Graham, and Taylor), R01-MH116782 (Wilson), R21-DC020270 (Heinrichs-Graham), R21-ES035146 (Taylor), and R01-EB020407 (Calhoun) from the National Institutes of Health, and grant #1539067 (Wilson, Calhoun, Wang, and Stephen) and #2112455 (Calhoun) from the National Science Foundation. The funders had no role in study design, data collection and analysis, decision to publish, or preparation of the manuscript. We want to thank the participants for volunteering to participate in the study and our staff and local collaborators for their contributions to the work.

Author contributions

T.W. Ward, M.S., and T.W. Wilson conceived the hypotheses. T.W. Wilson, E.H.G., B.K.T., M.S., V.D.C., Y.P.W., and J.M.S. obtained funding. G.C.E., D.L.R., A.T.C., and T.W. Wilson collected the data. M.S. and S.M.D. preprocessed the data. T.W. Ward and M.S. performed statistical analyses, wrote the manuscript, and prepared figures. T.W. Wilson, E.H.G., B.K.T., and Y.A. aided in interpretation of the results. All authors reviewed, provided feedback on, and approved the manuscript.

Competing interests

The authors declare no competing interests.

Ethical approval

All collaborators who have fulfilled the criteria for authorship required by Nature Portfolio journals have been included as authors for their essential contributions in designing and implementing the study. Roles and responsibilities were agreed upon among collaborators prior to the commencement of the research. This work includes findings that are locally relevant, which have been determined in collaboration with local partners. This research was not severely restricted or prohibited in the setting of the researchers, nor did our study procedures result in stigmatization, incrimination, discrimination, or personal risk to participants. Local and regional research relevant to our study was considered in the works cited.

Additional information

Supplementary information The online version contains supplementary material available at <https://doi.org/10.1038/s42003-024-06924-w>.

Correspondence and requests for materials should be addressed to Tony W. Wilson.

Peer review information *Communications Biology* thanks the anonymous reviewers for their contribution to the peer review of this work. Primary Handling Editor: Benjamin Bessieres. A peer review file is available.

Reprints and permissions information is available at <http://www.nature.com/reprints>

Publisher's note Springer Nature remains neutral with regard to jurisdictional claims in published maps and institutional affiliations.

Open Access This article is licensed under a Creative Commons Attribution-NonCommercial-NoDerivatives 4.0 International License, which permits any non-commercial use, sharing, distribution and reproduction in any medium or format, as long as you give appropriate credit to the original author(s) and the source, provide a link to the Creative Commons licence, and indicate if you modified the licensed material. You do not have permission under this licence to share adapted material derived from this article or parts of it. The images or other third party material in this article are included in the article's Creative Commons licence, unless indicated otherwise in a credit line to the material. If material is not included in the article's Creative Commons licence and your intended use is not permitted by statutory regulation or exceeds the permitted use, you will need to obtain permission directly from the copyright holder. To view a copy of this licence, visit <http://creativecommons.org/licenses/by-nc-nd/4.0/>.

© The Author(s) 2024